

1. Numerical Simulations of GIA-Induced Sea-Level Change

1.1. Methodology and Model Set-Up

Our predictions of ice-age sea-level change are based on a gravitationally self-consistent theory that accounts for time varying shorelines, the growth and retreat of grounded, marine-based ice sheets and the feedback into sea level of contemporaneous perturbations in the Earth's rotation vector¹. These numerical solutions, which are obtained up to spherical harmonic degree and order 256, require two inputs, the space-time geometry of the late Pleistocene ice cover and the viscoelastic structure of the adopted Earth model. We describe each of these inputs, in turn, below.

Our ice model is constructed by combining a global stack of benthic $\delta^{18}\text{O}$ records² with the geometry of the ICE-5G ice model³ for the last glacial cycle. To begin, we convert the global $\delta^{18}\text{O}$ stack into a variation in eustatic (i.e., globally uniform) sea-level (ESL) using a simple linear scaling calibrated to match the total change in ESL across the last glacial cycle (~130 m). Since our purpose here is to estimate interglacial sea-level changes due to glacial isostatic adjustment (GIA), the time series is clipped such that whenever the $\delta^{18}\text{O}$ value falls below the modern value, ESL is set to 0. That is, we never allow ice volumes to be less than present-day volumes. For the last glacial cycle alone, the scaled ESL time series is replaced by the ESL curve for the ICE-5G ice history³. The resulting trend in ESL is shown in Figure S1 (black line). Note that during the MIS 11 interglacial, the clipping procedure yields a period of constant ice volume (equal to the present-day) that

extends 9 kyr, from 410 kyr to 401 kyr. Finally, the ESL curve in Figure S1 is converted to an ice sheet history by assuming that at any time that ESL matches a snapshot of ESL in the ICE-5G model, the geometry of the ice cover is identical to the associated ICE-5G geometry.

In regard to the second input, we adopt a spherically symmetric (i.e., depth-varying), self-gravitating, Maxwell viscoelastic rheology. The density and elastic structure of the Earth model is discretized into about 200 layers with values taken from the seismic model PREM⁴. The radial viscosity profile adopted in computing Figures 2-4 of the main text is comprised of three layers: an infinite viscosity (i.e., elastic) lithosphere of thickness 90 km, a sub-lithospheric upper mantle of viscosity 5×10^{20} Pa s, and a lower mantle of viscosity 5×10^{21} Pa s (henceforth model LM). This lower mantle viscosity is at the lower bound of a series of inferences based on data sets related to ice age dynamics⁵, including a joint inversion of these data sets with observables related to mantle convection⁶.

In the results below, and in the main text, we present predictions based on two other viscosity models: model LM2 which is identical to model LM with the exception that the lower mantle viscosity is increased to 10^{22} Pa s; and model VM2 (ref. 3) which is based on an analysis of GIA data, has an elastic lithosphere of thickness 90 km, and a multi-layer mantle viscosity profile with mean values of $\sim 4\text{-}5 \times 10^{20}$ Pa s in the upper mantle and $\sim 2 \times 10^{21}$ Pa s in the lower mantle. We also report below on a statistical study in which the lithospheric thickness, upper and lower mantle viscosity are varied across a wide range as part of a Monte-Carlo based analysis of MIS 11 sea-level records.

1.2. Simulations Based on Model LM

As discussed in the main text, numerical calculations based on model LM reveal two geographic zones with distinct GIA-induced highstand amplitudes and time histories (Figures 2-4). Within the peripheral bulges of ancient ice cover, relatively large amplitude highstands would date to the end of the interglacial hiatus in ice mass changes. In contrast, at far-field sites, smaller amplitude highstands date to the beginning of the hiatus.

In the first zone, which includes Bermuda and Bahamas, the current elevation of a MIS 11 sea-level marker depends on the difference between the level of isostatic disequilibrium at the end of the protracted MIS 11 hiatus and at present day. The longer the duration of the MIS 11 hiatus in ice mass changes, the greater the present elevation of the ancient shoreline since, in this case, a site on the peripheral bulge would have experienced progressively more relative sea-level rise during the MIS 11 interglacial than during the current interglacial (due to the fact that it was subsiding longer). Thus, in the absence of any future changes in global ice volume (such as would occur at the onset of a new glaciation phase), ongoing GIA-induced subsidence and associated sea-level rise in Bermuda and Bahamas would lead to a continuing, monotonic reduction in the elevation of the MIS 11 highstands.

In the second zone, which includes the far field of the late Pleistocene ice sheets (Figures 2-4), highstands will date to the beginning of the hiatus in ice volume changes associated with the model MIS 11 interglacial. The highstand elevation at such sites reflects the difference in isostatic disequilibrium at the beginning of the interglacial hiatus relative

to the isostatic disequilibrium at present day, and therefore this elevation does not depend on the duration of the ancient interglacial. As the current interglacial proceeds, sea level due to glacial isostatic adjustment will fall at these far-field sites and thus the ancient highstand amplitude will (ignoring modern instability of the polar ice sheets) progressively increase.

1.3. Sensitivity Analysis

We next explore the sensitivity of the GIA predictions for Bermuda and Bahamas to variations in either the viscoelastic structure of the Earth model or the assumed duration of the model MIS 11 highstand. Figure 2 in the main text is the predicted sea-level change across the 9 kyr hiatus in ice volume changes (410–401 kyr) in the model MIS 11 interglacial. The figure is based on the viscosity model LM, and in Figure S2 we repeat the calculation using models (a) VM2 and (b) LM2. The amplitude of the predicted sea-level change within the peripheral bulge regions is clearly sensitive to the adopted viscosity profile. A comparison of Figure 2 with Figure S2a indicates that a relatively modest, factor of ~ 2 , increase in lower mantle viscosity from model VM2 to model LM yields a factor of two increase in the predicted peak sea-level change within the peripheral bulge. This increase suggests that calculations based on model VM2 are closer to equilibrium by the start of the model MIS 11 interglacial (i.e., 410 kyr) than predictions based on model LM. In contrast, comparison of Figures 2 and S2b indicates that the GIA-induced sea-level predictions are less sensitive to any further increase in viscosity. We note that predictions of the sea-level change in the far field of the former MIS 12 ice sheets are relatively insensitive, in an absolute sense, to variations in the adopted viscosity profile.

In Table S1, we consider the impact of varying mantle viscosity and the assumed duration of the model MIS 11 interglacial on highstand predictions at Bermuda and Bahamas. The second column in Table S1 lists the published highstand estimates for these two sites. The third through fifth column are our GIA-corrected estimates, where the corrections are based on a 9 kyr hiatus in ice volume changes and the LM, VM2 and LM2 viscosity models, respectively. As the lower mantle viscosity is progressively decreased, the peripheral bulges are predicted to have relaxed closer to isostatic equilibrium at the end of both the MIS 11 and present interglacial. Therefore, the predicted difference between the level of disequilibrium at these two times, which governs the predicted highstand elevation, is reduced.

In the next three columns of Table S1, we repeat the above predictions but now adopt a hiatus in MIS 11 ice sheet melt or growth that extends from 415-401 kyr. The calculation based on the more protracted interglacial predicts GIA contributions to the highstands of even greater amplitude at peripheral bulges sites such as Bermuda and Bahamas. This trend is expected given that the difference in the predicted level of isostatic disequilibrium between the end of MIS 11 and the present will increase as the duration of the model MIS 11 interglacial is lengthened. Specifically, the increase in predicted highstand amplitude when the longer duration is adopted is ~1-2 m for calculations adopting viscosity model LM, leading to a decrease of the same amount in the GIA-corrected highstand elevations. This impact drops to ~0.5 m or less when the VM2 viscosity profile is used in place of model LM, and increases to ~2-4 m in calculations based on model LM2.

As discussed in the main text, the GIA correction to sea level at the end of the model MIS 11 interglacial and at far-field sites is, using viscosity profile LM and a 9 kyr hiatus in ice volume changes, ~ 1 m. This correction is relatively insensitive to the choice of viscosity and it is insensitive to the duration of the hiatus, and using any of the six cases considered in Table S1 will vary the mean far-field GIA correction by ~ 0.5 m.

1.4. Monte-Carlo Analysis of Peak ESL During MIS 11

We derive a preferred range for the peak eustatic sea-level during MIS 11 on the basis of a Monte-Carlo search through the GIA model parameter space. In this exercise, we adopt the following observational constraints on MIS 11 highstand elevations (with associated $2\text{-}\sigma$ error bars): (1) Bermuda, 21.3 ± 1.0 m (ref. 7); (2) Bahamas, 18.5 ± 3.6 m (ref. 8); and (3) 7.6 ± 3.5 m (mean) at the far-field sites in the Bowen⁹ review. We perform a large suite of ice age sea-level calculations in which the following parameters are varied: upper and lower mantle viscosity in the range $0.3\text{--}1.0 \times 10^{21}$ Pa s and $1\text{--}100 \times 10^{21}$ Pa s, respectively, lithospheric thickness in the range 70–120 km, and the duration of the hiatus in model MIS 11 ice volume changes from 6 kyr to 14 kyr (where all time windows are assumed to end at 401 kyr). Each simulation yields GIA-induced MIS 11 highstand elevations at the sites of interest and to these predictions we add a tectonic signal modelled as a random variable with uniform probability distribution in the range [−1m, 1m]. This total (GIA plus tectonic) prediction is then used to correct the observational constraints, and the three residual highstands are tested for consistency by computing the χ^2 misfit about their mean. Figure S3 shows the minimum misfit as a function of peak ESL during MIS 11,

where the latter is estimated by the mean of the three corrected observations. (Melting of polar ice sheets to account for these corrected observations would lead to sea-level change that is characterized by geographic variability. Test calculations indicate that the mean of the three corrected observations will be within ~ 1 m of the actual ESL.) We note that no GIA prediction computed using the suite of Earth models and event duration listed above brought the mean corrected highstand value below 6 m, and this serves as a hard lower bound on the peak ESL during MIS 11. Using an F-test for the significance of a χ^2 misfit above the global minimum value yields a 99% confidence interval of 6–13 m for the peak ESL during MIS 11.

As a final point, the importance of the GIA correction to the interpretation of observations at Bermuda and Bahamas does not depend on the veracity of the far-field records (which show high variability). Even if we were to ignore these records, a GIA correction based on an Earth model with a weak lower mantle (e.g., VM2) still corrects the Bermuda and Bahamas observations down to 14–15 m (Table S1), which is only marginally higher than the upper bound we have derived on the basis of the Monte-Carlo search. So, in that sense, our upper bound on the peak ESL during MIS 11 (i.e., 13 m) is also a reasonably hard bound.

1.5. Comparison of the Duration of Interglacials MIS 5e and MIS 11

In Figure 1 of the main text, we compare the relative duration of the MIS 11 and the current interglacial by superimposing the LR04 benthic oxygen isotope stack² over the two periods. In Figure S4 we provide an analogous comparison of the duration of the MIS 11 and MIS 5e interglacials.

References:

1. Kendall, R. A., Mitrovica, J. X. & Milne, G. A. On post-glacial SL: II. Numerical formulation and comparative results on spherically symmetric models. *Geophys. J. Int.* **161**, 679-706 (2005).
2. Lisiecki, L. E. & Raymo, M. E. A Pliocene-Pleistocene stack of 57 globally distributed benthic $\delta^{18}\text{O}$ records. *Paleoceanography* **20**, PA1003, doi:10.1029/2004PA001071 (2005).
3. Peltier, W. R. Global glacial isostasy and the surface of the ice-age Earth: The ICE-5G (VM2) model and GRACE. *Ann. Rev. Earth Planet. Sci.* **32**, 111-149 (2004).
4. Dziewonski, A. M. & Anderson, D. L. Preliminary reference Earth model (PREM). *Phys. Earth Planet. Int.* **25**, 297-356 (1981).
5. Lambeck, K., Smither, C. & Johnston, P. Sea level change, glacial rebound and mantle viscosity for northern Europe. *Geophys. J. Int.* **134**, 102-144 (1998).
6. Mitrovica, J. X. & Forte, A. M. A new inference of mantle viscosity based upon a joint inversion of convection and glacial isostatic adjustment data. *Earth Planet. Sci. Lett.* **225**, 177-189 (2004).
7. Olson, S. L. & Hearty, P. A sustained +21 m sea level highstand during MIS 11 (400 ka): direct fossil and sedimentary evidence from Bermuda. *Quaternary Science Reviews* **28**, 271-285 (2009).
8. Hearty, P. J., Kindler, P., Cheng, H. & Edwards, R. L. A +20 m middle Pleistocene sea level highstand (Bermuda and the Bahamas) due to partial collapse of Antarctic ice. *Geology* **27**, 375-378 (1999).
9. Bowen, D. Q. Sea level ~400000 years ago (MIS 11): analogue for present and future sea-level? *Clim. Past* **6**, 19-29 (2010).

Table S1. Observed and GIA-corrected MIS 11 highstand elevation. GIA corrections are computed at 401 kyr, and are based on three different mantle viscosity models (LM, VM2 and LM2) and two choices for MIS 11 duration (9 kyr and 14 kyr).

Study Site	MIS11 SL (m)*	LM (9kyr) (m)	VM2 (9kyr) (m)	LM2 (9kyr) (m)	LM (14kyr) (m)	VM2 (14kyr) (m)	LM2 (14kyr) (m)
Bermuda ⁷	21.3±1	9.4	15.0	8.4	7.0	14.5	4.3
Eleuthera, Bahamas ⁸	18.5±3.6	11.1	14.3	9.8	9.9	14.1	7.5

*See text as well as original studies for discussion of observationally-determined errors on field data.

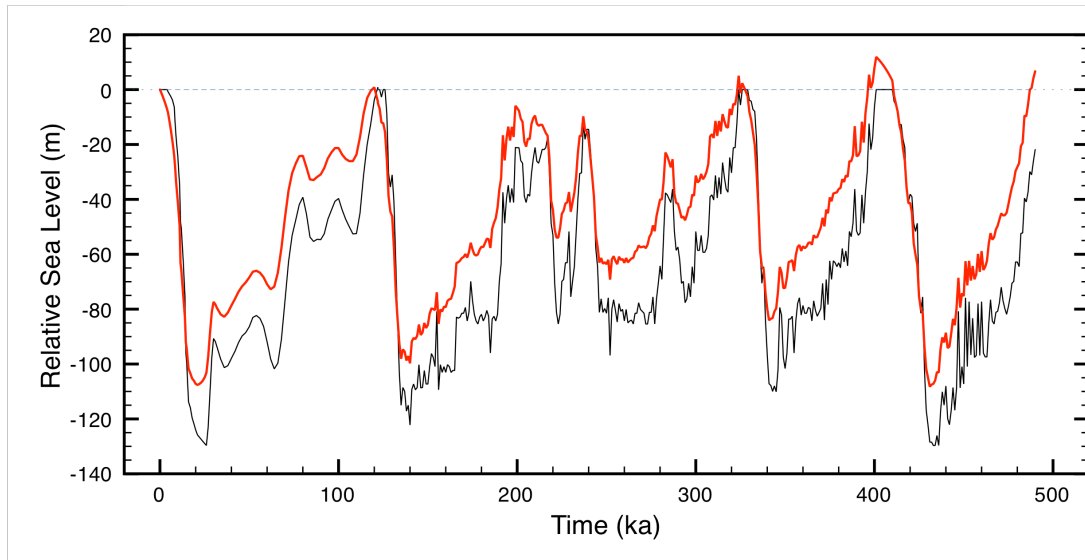


Figure S1: Relative SL sea-level variations over the last 500 kyr. Solid black line – eustatic sea-level change over the last 500 kyr associated with the model ice history adopted in the numerical simulations (see text). Red line – relative sea-level history for Bermuda predicted on the basis of this ice history and the LM viscosity model. Note the 9 kyr hiatus in the model ice volume history during MIS 11 (410-401 kyr) and the long duration of this interglacial relative to both the Holocene (see also Figure 1 of the main text) and MIS 5e (Figure S4 below).

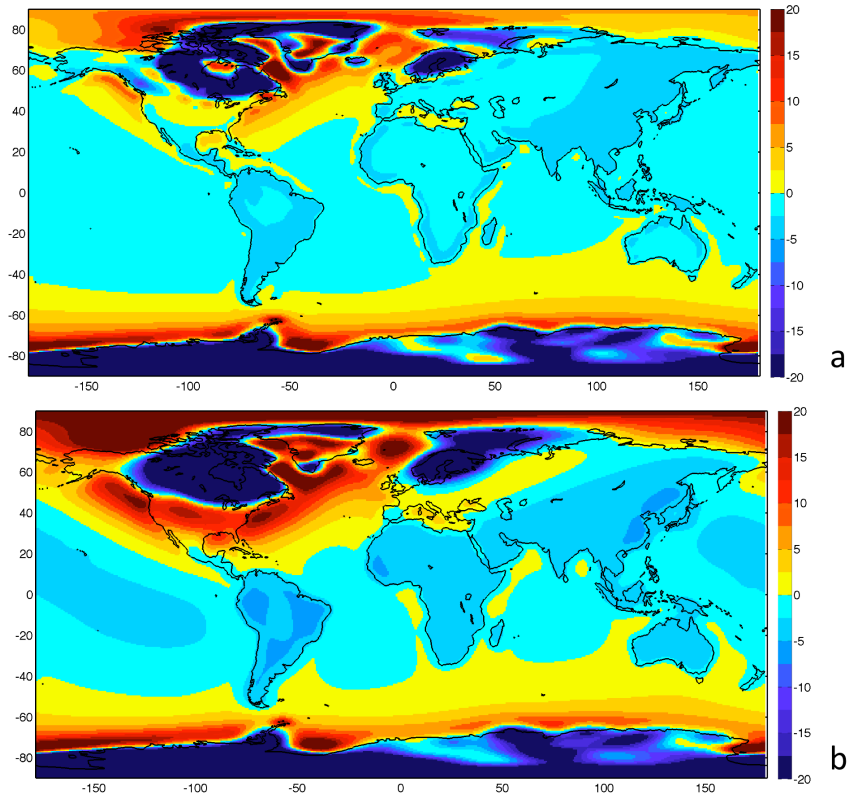


Figure S2. Predicted sea-level change (m) across the hiatus in ice volume changes (410 – 401 kyr) spanned by the model MIS 11 interglacial. The GIA calculation is based on the ice history discussed in the text and the (a) VM2 and (b) LM2 viscosity models. The colour scale saturates in regions within the near field of the late Pleistocene ice sheets.

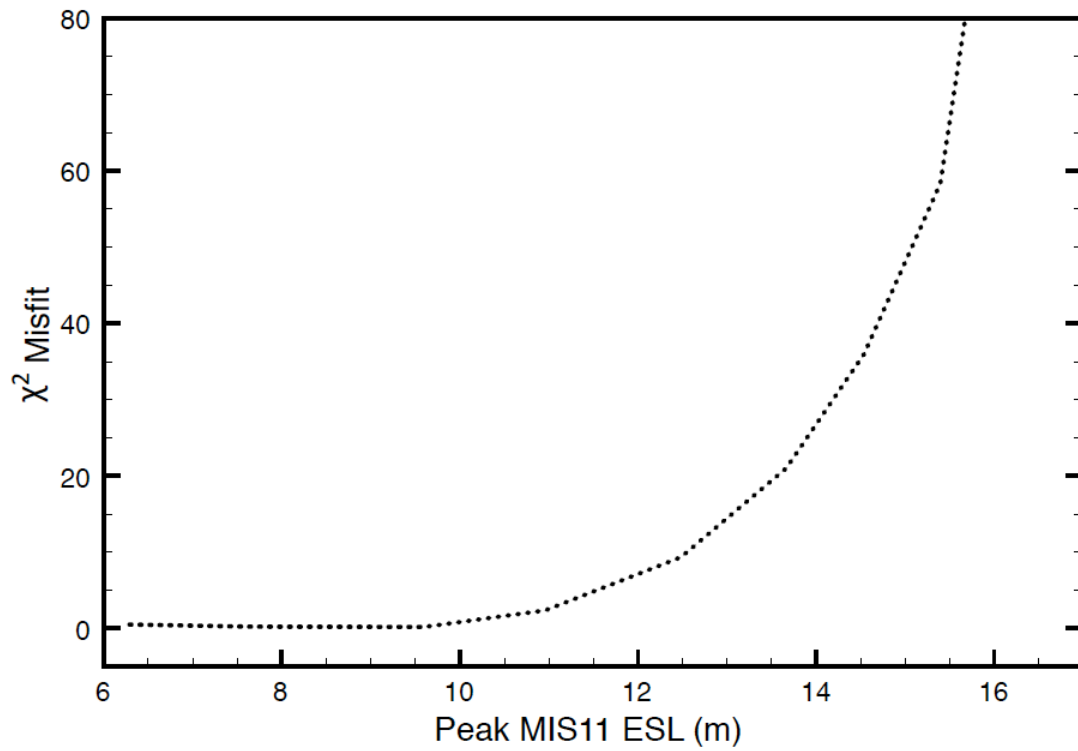


Figure S3. Results of Monte Carlo analysis showing the minimum χ^2 misfit as a function of peak eustatic sea level during MIS 11.

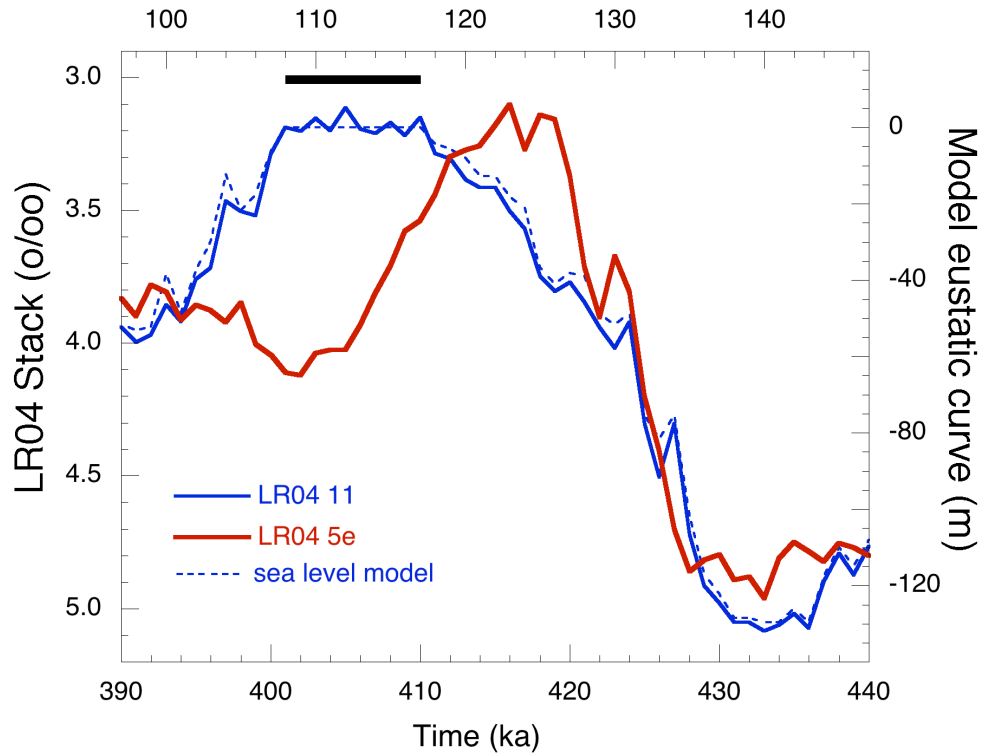


Figure S4. Comparison of the duration of the MIS 11 and MIS 5e interglacials. Plot of the LR04 benthic oxygen isotope stack² (in units of ‰ VPDB, left axis) over a time window spanning the MIS 11 (blue; bottom time scale) and MIS 5e (red; top time scale) interglacials. The mean standard error on $\delta^{18}\text{O}$ in the LR04 stack is 0.06‰ with an age error of ± 4 kyr for the intervals considered here. The juxtaposition illustrates the significantly longer duration of interglacial conditions during MIS 11 relative to MIS 5e. Eustatic sea level associated with the model ice history used to calculate GIA effects during MIS 11 is shown by the dashed line (right axis).